Leibniz Gemeinschaft

WIAS

Weierstrass Institute for Applied Analysis and Stochastics

in Forschungsverbund Berlin e.V., Mohrenstrasse 39, D - 10117 Berlin, Germany

Fluidyzacja ośrodków granulowanych – eksperyment i model

KRZYSZTOF WILMAŃSKI

mail: wilmansk@wias-berlin.de

web : http://www.wias-berlin.de/people/wilmansk

Wykład w Zakładzie Mechaniki i Fizyki Płynów
Instytut Podstawowych Problemów Techniki PAN
Warszawa, 10 marca, 2004

Liquefaction and other ground instabilities

Ground rupture (Taiwan)

Landslide in El Salvador (Colonia Las Colinas) by the earthquake 13.01.2001

Adapazari

Taiwan

Tilt due to liquefaction (Adapazari)

Liquefaction (Monterey)

Liquefaction (Kobe)

Tilt due to liquefaction (Kobe)

Catastrophic cosequences of liquefaction – toppled houses due to liquefaction after the Niigata earthquake, Japan 1964

Damage due to liquefaction during the earthquake in Niigata, Japan 1964: Sunk truck (left) and floated up sewage tank (right).

Eruption of pore water after an underground explosion

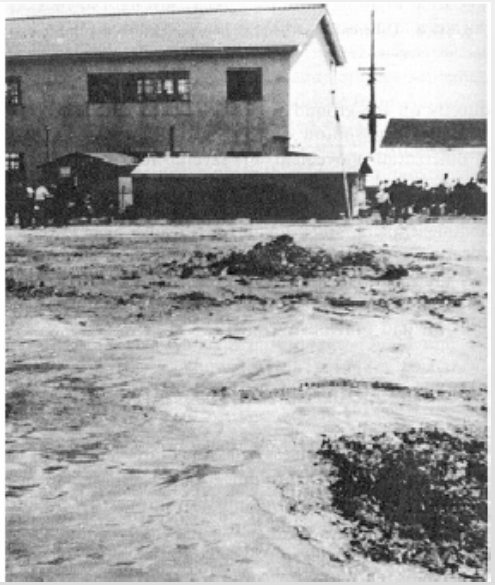

Eruption of sand (slurry) volcano during the Niigata earthquake in Japan 1964

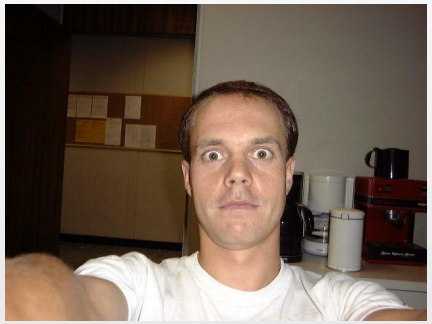

Experiments on a saturated sand

PhD-Thesis: Theo Wilhelm, University of Innsbruck, 2000

Theo Wilhelm, K. Wilmanski; *On the Onset of Flow Instabilities in Granular Media due to Porosity Inhomogeneities, Int. J. Multiphase Flows,* **28**, 1929-1944, 2002.

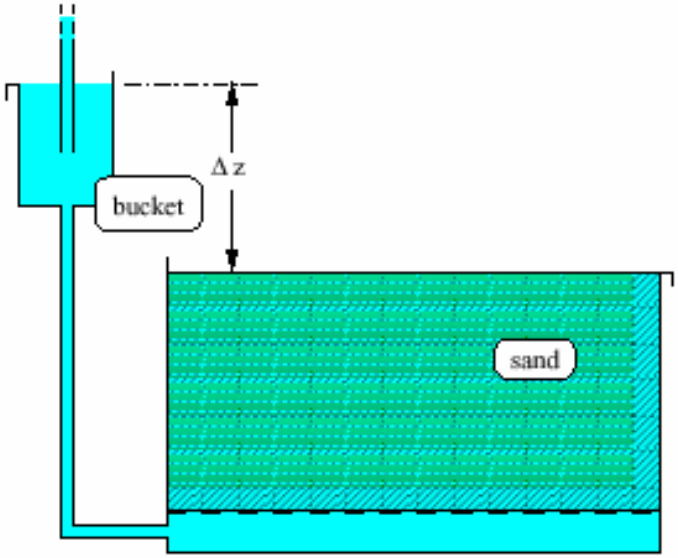

Experimental setup

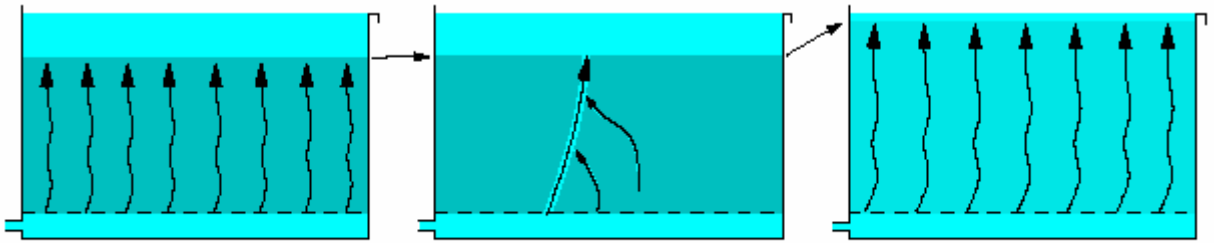

Flow regimes in sand-water mixtures under seepage conditions

1. Hemogeneously distributed micro-channels (small dark spots) on the top surface of a sand speciment subject to seepage. Diameters of channels up to 1 mm.

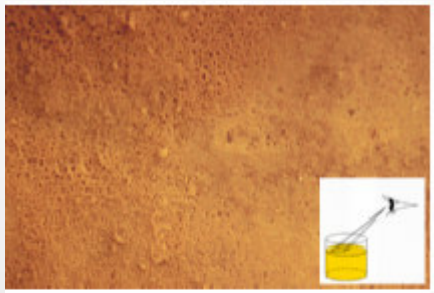

2. Channels with diameters up to several mm have formed. Very fine particles flushed out through them are visible in the water layer above the sand surface.

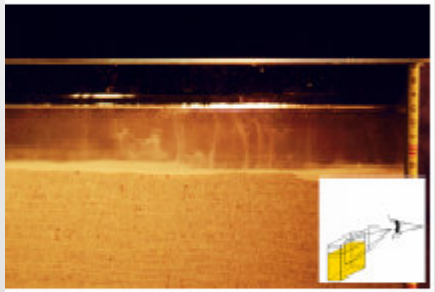

3. Instabilities (washed out air bubbles, erupting channels) shortly before the eruption of a main channel.

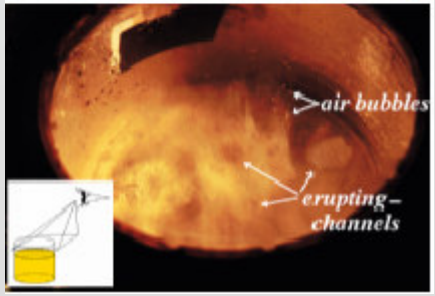

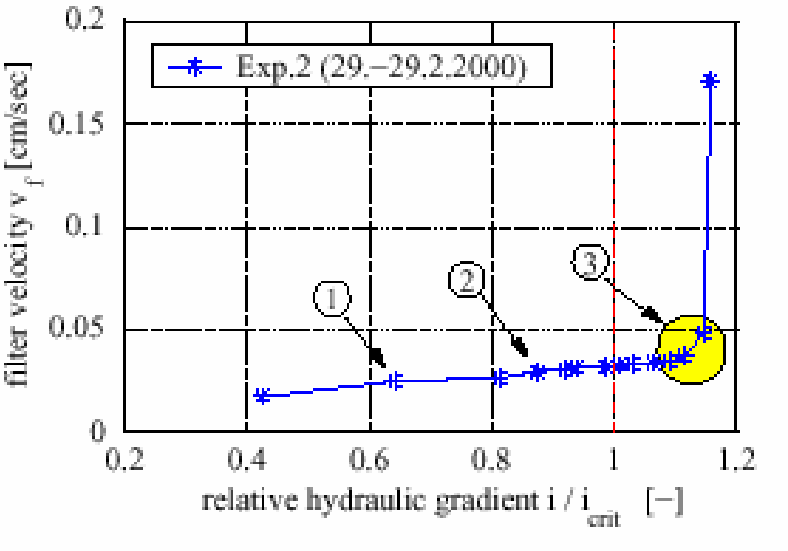

Experimental data from a seepage experiment.

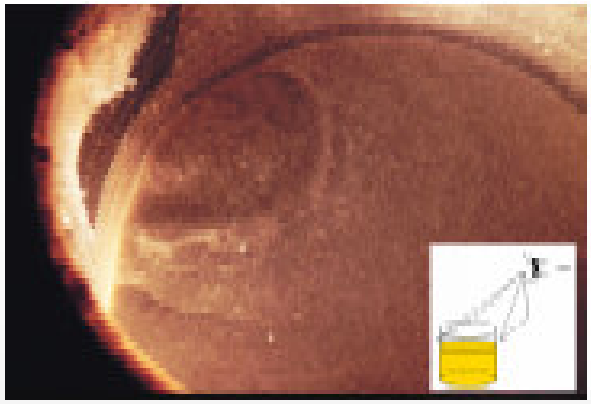

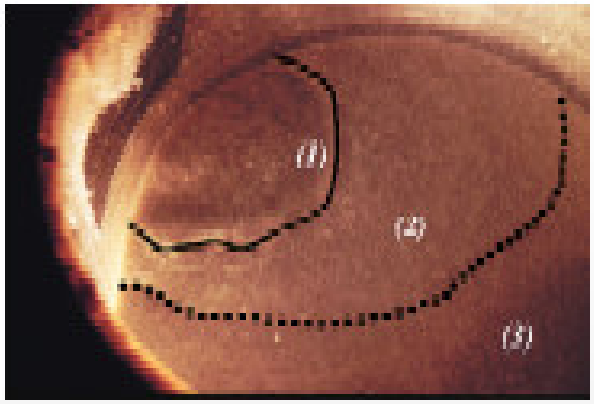

Channel erupting on the surface. Regions marked in the right figure: (1) Channel; (2) Fluidized region; (3) Stable region.

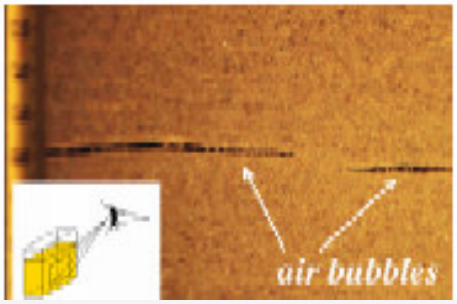

Filter instability (left) and air bubbles trapped in horizontal barriers of very fine particles

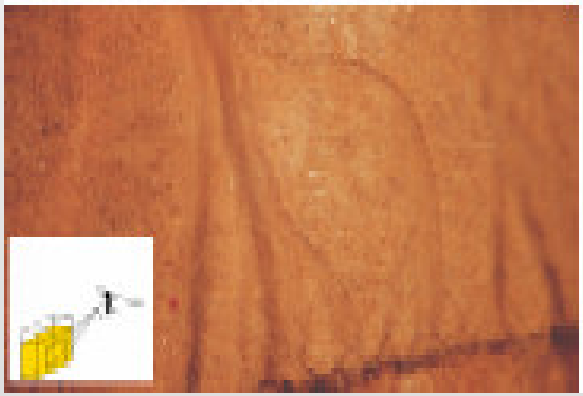

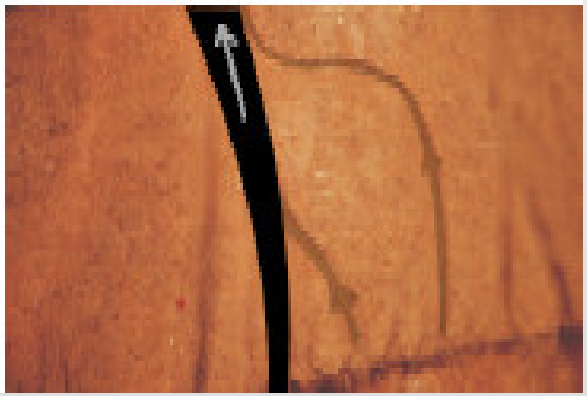

A main channel (indicated by the dark shadow in the right figure) is fed by two smaller channels (indicated by the light grey areas in the right figure). Both smaller channels changed their direction due to the attraction of the main channel

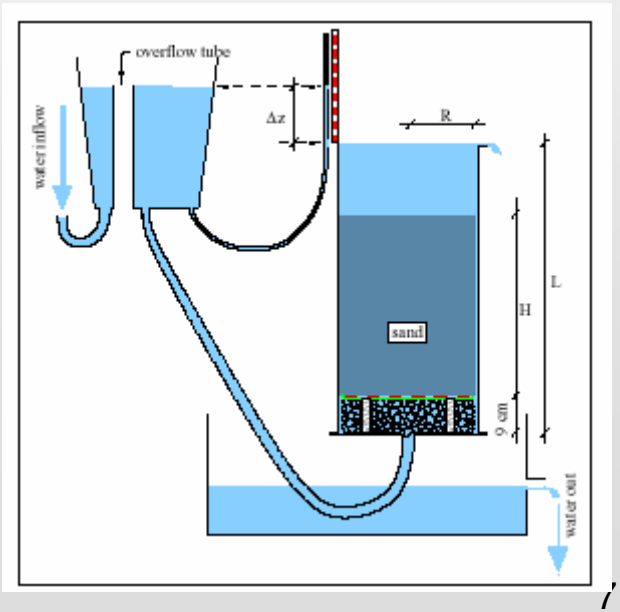

Experimental setup

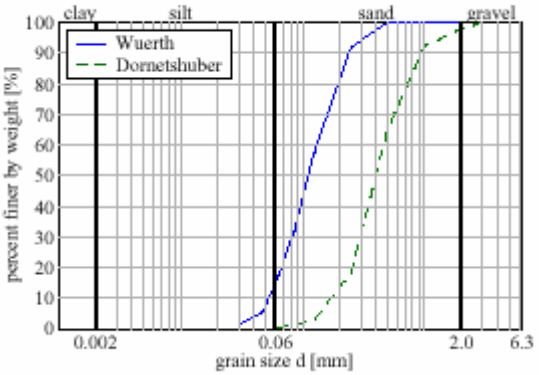

Grain distribution curves of Feinsand Wuerth and Sand Dornetshuber

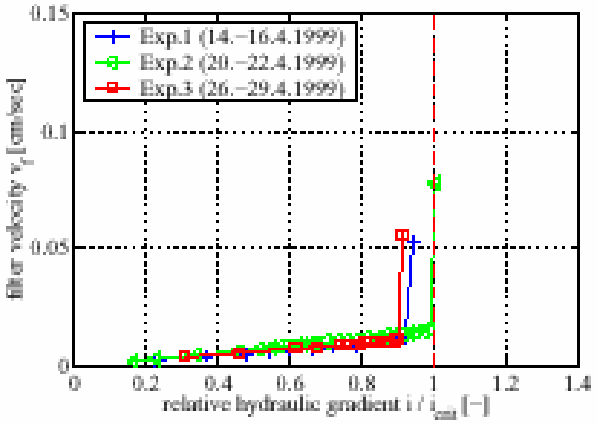

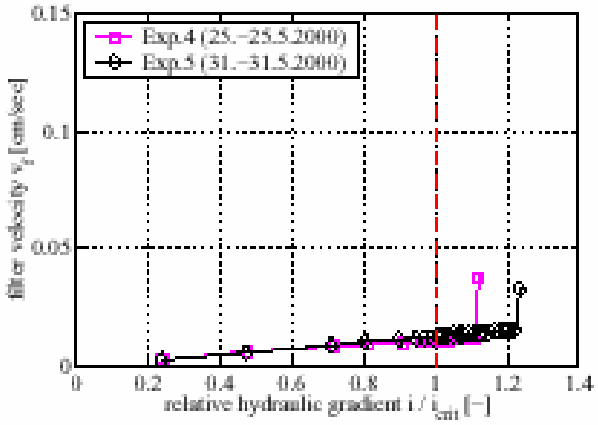

Filter velocity v_f versus relative hydraulic gradient i/i_{crit} for Feinsand Wuerth in initially medium to dense packing (left) and dense packing (right).

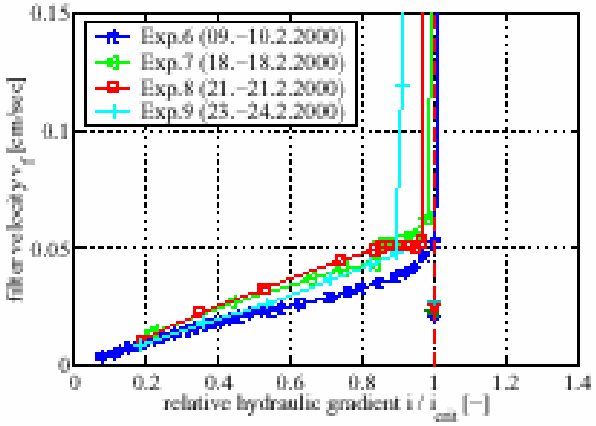

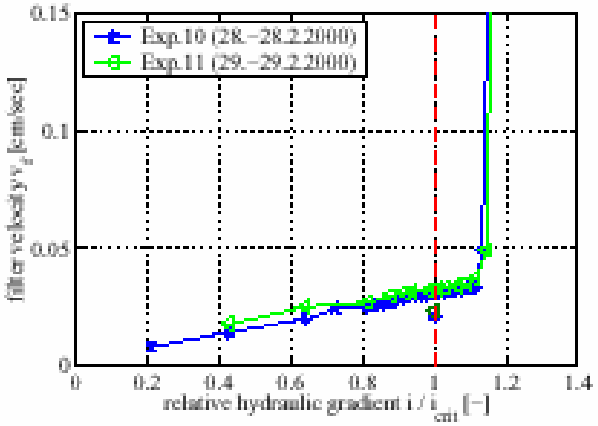

Filter velocity v_f versus relative hydraulic gradient i/i_{crit} for Sand Dornetshuber in initially medium packing (left) and initially dense packing (right).

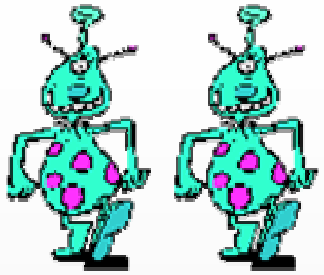

Two-component model of the porous saturated medium with a dependence on the porosity gradient.

Fields: $(\mathbf{x},t)\to\{\rho^S,\rho^F,n,u_k^S,v_k^S\},\quad k=1,2,3.$

ρ^S - partial mass density of the skeleton,

ρ^F - partial density of the fluid,

n - porosity (volume fraction of the fluid in REV,

u_k^S - displacement of the skeleton,

v_k^F - velocity of the fluid.

Auxiliary quantities:

$$w_k := v_k^F - v_k^S,\quad v_k^S := \frac{\partial u_k^S}{\partial t},$$ - seepage velocity,

ρ^{SR},ρ^{FR} - true (real) mass densities.

$$\rho^S=(1-n)\rho^{SR},\quad \rho^F=n\rho^{FR}.$$

Partial balance equations:

Mass balance:

$$\frac{\partial \rho^S}{\partial t} + \frac{\partial}{\partial x^k}\left(\rho^S v_k^S\right) = \hat{\rho}^S, \quad \frac{\partial \rho^F}{\partial t} + \frac{\partial}{\partial x^k}\left(\rho^F v_k^F\right) = \hat{\rho}^F,$$

Momentum balance:

$$\frac{\partial \rho^S v_k^S}{\partial t} + \frac{\partial}{\partial x^l}\left(\rho^S v_k^S v_l^S - T_{kl}^S\right) = \hat{p}_k,$$

$$\frac{\partial \rho^F v_k^F}{\partial t} + \frac{\partial}{\partial x^l}\left(\rho^F v_k^F v_l^F - T_{kl}^F\right) = -\hat{p}_k,$$

Integrability (linear – existence of displacement):

$$\frac{\partial e_{kl}}{\partial t} = \frac{1}{2}\left(\frac{\partial v_k^S}{\partial x^l} + \frac{\partial v_l^S}{\partial x^k}\right) \quad \Rightarrow \quad \exists u_k^S : v_k^S = \frac{\partial u_k^S}{\partial t},\ e_{kl} = \frac{1}{2}\left(\frac{\partial u_k^S}{\partial x^l} + \frac{\partial u_l^S}{\partial x^k}\right).$$

Assumptions: - no mass sources,

$$\hat{\rho}^S = \hat{\rho}^F = 0,$$

- incompressibility of true components, i.e.

$$\rho^{SR} = const., \quad \rho^{FR} = const.$$

Then new unknown fields:

$$\left(x^k, t\right) \rightarrow \left\{n, p, u_k^S, v_k^F\right\},$$

p - reaction pressure.

Treshold behavior w.r.t. the porosity gradient. Dependence of material parameters on the current porosity singular at the critical seepage velocity.

Partial mass balance equations can be written in the form

$$\frac{\partial n}{\partial t} + \frac{\partial}{\partial x^k}\left(n v_k^F\right) = 0, \quad -\frac{\partial n}{\partial t} + \frac{\partial}{\partial x^k}\left((1-n) v_k^S\right) = 0 \quad \Rightarrow \quad \frac{\partial}{\partial x^k}\left[n v_k^F + (1-n) v_k^S\right] = 0.$$

The third relation is the constraint relation for the incompressibility.

Constitutive relations for poroelastic materials

Assumption: linear elasticity, ideal fluid, threshold through dependence on porosity gradient

Partial stress tensors and the momentum source:

$$T^S_{kl} = -(1-n)p\delta_{kl} + \lambda^S e_{mm}\delta_{kl} + 2\mu^S e_{kl},$$

$$T^F_{kl} = -np\delta_{kl},$$

$$\hat{p}_k = \Pi w_k - \left(p + \rho^S \frac{\partial \psi^S}{\partial n} \right) \frac{\partial n}{\partial x^k}.$$

Dependence of free energies on porosity and relative velocity (**thermodynamics**):

$$\rho^S \frac{\partial \psi^S}{\partial n} = -\rho^F \frac{\partial \psi^F}{\partial n} = \frac{\Gamma}{\sqrt{2}} \left(1 + \frac{W-Y}{|W-Y|} \right) \sqrt{W}, \quad W := \tfrac{1}{2} w_m w_m, \quad \Gamma, Y > 0.$$

- threshold behavior: $\sqrt{2Y}$ - critical seepage velocity.

Thermodynamical identity (integrability condition):

$$\frac{\partial}{\partial e_{kl}} \left(\frac{\rho^F \psi^F}{n} - \frac{\rho^S \psi^S}{1-n} \right) = \frac{\partial}{\partial n} \left(\lambda^S e_{mm}\delta_{kl} + 2\mu^S e_{kl} \right).$$

Field equations for fields: $\{n, p, e_{kl}, v_k^S, v_k^F\}$

$$\frac{\partial n}{\partial t}+\frac{\partial}{\partial x^k}\left(n v_k^F\right)=0, \quad \frac{\partial}{\partial x^k}\left[n v_k^F+(1-n) v_k^S\right]=0.$$

$$\frac{\partial e_{kl}}{\partial t}=\tfrac{1}{2}\left(\frac{\partial v_k^S}{\partial x^l}+\frac{\partial v_l^S}{\partial x^k}\right).$$

$$\rho^S\left(\frac{\partial v_k^S}{\partial t}+v_l^S\frac{\partial v_k^S}{\partial x^l}\right)=-(1-n)\frac{\partial p}{\partial x^k}+\frac{\partial}{\partial x^l}\left(\lambda^S e_{mm}\delta_{kl}+2\mu^S e_{kl}\right)+$$
$$+\Pi w_k-\frac{\Gamma}{\sqrt{2}}\left(1+\frac{W-Y}{|W-Y|}\right)\frac{\partial n}{\partial x^k}+\rho^S g_k,$$

$$\rho^F\left(\frac{\partial v_k^F}{\partial t}+v_l^F\frac{\partial v_k^F}{\partial x^l}\right)=-n\frac{\partial p}{\partial x^k}-\Pi w_k+\frac{\Gamma}{\sqrt{2}}\left(1+\frac{W-Y}{|W-Y|}\right)\frac{\partial n}{\partial x^k}+\rho^F g_k,$$

$$w_k:=v_k^F-v_k^S, \quad W:=\tfrac{1}{2}w_m w_m.$$

material parameters: $\{\lambda^S, \mu^S, \Pi, \mathrm{Y}, \Gamma\}$

Plane deformation – 1D case:

$$\frac{\partial n}{\partial t}+\frac{\partial}{\partial z}\left(nv^F\right)=0,\quad -\frac{\partial n}{\partial t}+\frac{\partial}{\partial z}\left((1-n)nv^S\right)=0,\quad v^F:=v_3^F,\quad v^S:=v_3^S,\quad z:=x^3,$$

$$n\rho^{FR}\left(\frac{\partial v^F}{\partial t}+v^F\frac{\partial v^F}{\partial z}\right)=-n\frac{\partial p}{\partial z}+n\rho^{FR}g-\Pi\left(v^F-v^S\right)+\Gamma\left|v^F-v^S\right|\frac{\partial n}{\partial z},$$

$$(1-n)\rho^{SR}\left(\frac{\partial v^S}{\partial t}+v^S\frac{\partial v^S}{\partial z}\right)=E\frac{\partial e}{\partial z}-(1-n)\frac{\partial p}{\partial z}+(1-n)\rho^{SR}g+\Pi\left(v^F-v^S\right)-\Gamma\left|v^F-v^S\right|\frac{\partial n}{\partial z},$$

$$\frac{\partial e}{\partial t}=\frac{\partial v^S}{\partial z},\quad e:=e_{33}\quad E:=\lambda^S+2\mu^S.$$

Ground state – homogeneous seepage:

$$n=n_0=const.,\quad v^S=v_0^S=0,\quad v^F=v_0^F=const,$$

$$e=e_0=-\frac{\gamma'_0}{E}z,\quad p=p_0(z).$$

$$\Rightarrow\quad \gamma'_0=(1-n_0)\left(\rho^{SR}-\rho^{FR}\right)g\quad \text{- submerged weight of the skeleton}$$

$$\mathrm{E}e_0=-\gamma'_0 z,\quad p_0=\rho^{FR}gz.$$

Small perturbation – wave ansatz:

$$n_1 = N\mathcal{E}, \quad v_1^S = V^S\mathcal{E}, \quad v_1^F = V^F\mathcal{E}, \quad p_1 = P\mathcal{E}, \quad e_1 = B\mathcal{E},$$
$$\mathcal{E} := \exp(st + ikz).$$

Eigenvalue problem:

$$\det \mathbf{A} = 0,$$

$$\mathbf{A} := \begin{pmatrix} s + v_0^F ik & 0 & n_0 ik & 0 & 0 \\ -s & (1-n_0)ik & 0 & 0 & 0 \\ \frac{\partial p_0}{\partial z} - \rho^{FR} g - \Gamma\left|v_0^F\right| ik & -\Pi & n_0\rho^{FR} s + \Pi & n_0 ik & 0 \\ -\frac{\partial p_0}{\partial z} + \rho^{SR} g + \Gamma\left|v_0^F\right| ik & (1-n_0)\rho^{SR} s + \Pi & -\Pi & (1-n_0)ik & -Eik \\ 0 & -ik & 0 & 0 & s \end{pmatrix}$$

Numerical evaluation for the data:

$$\rho^{SR} = 2650\,kg/m^3, \quad \rho^{FR} = 1000\,kg/m^3,$$
$$n_0 = 0.47, \quad \Pi = 1.2\times 10^7\,kg/m^3/s,$$
$$v_0^F = -1.6\times 10^{-4}\,m/s, \quad \frac{\partial p_0}{\partial z} = 14085\,Pa/m.$$

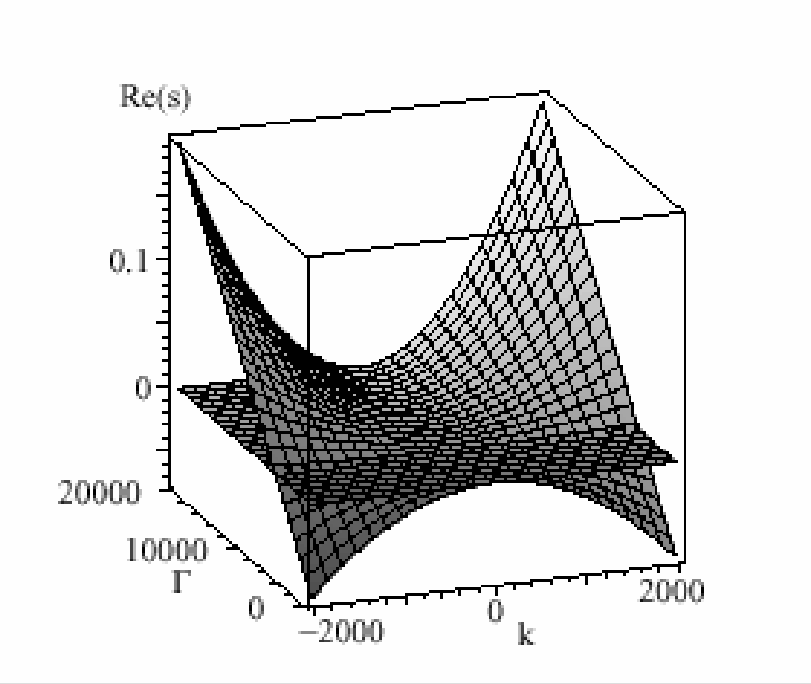

Positive real part of *s* determines the range of instability

Concluding remarks

1) The model predicts the onset of instability but not its evolution,

2) Improvement would require the full nonlinearity (e.g. dependence of parameters on porosity),

3) Unsuccessful attempt to apply hypoplasticity – - indication that microde--formations of skeleton may be immaterial.